Electrochemical and Solid-State Letters, **6** (2) G22-G24 (2003)
0013-4651/2002/6(2)/G22/3/$7.00 © The Electrochemical Society, Inc.

Structural and Electrical Characterization of Porous Silicon Carbide Formed in n-6H-SiC Substrates

S. Soloviev, T. Das,[z] and T. S. Sudarshan

Department of Electrical Engineering, University of South Carolina, Columbia, South Carolina 29208, USA

Investigation of porous silicon carbide layer morphology and its growth rate was studied along with electrical characterization. Morphology of the formed porous SiC layers was analyzed by scanning electron microscopy. The effective carrier density in porous layers was extracted from the capacitance-voltage characteristics of mercury probe Schottky contacts to the porous layer. It was found that the effective carrier density in porous layer and the pore density are in good correlation.
 [DOI: 10.1149/1.1534733]

Manuscript submitted April 16, 2002; revised manuscript received August 30, 2002. Available electronically December 12, 2002.

The wide bandgap of silicon carbide (SiC) semiconductor gives it the edge over other materials for making high power, high temperature, and high frequency devices. High thermal conductivity, saturation electric drift velocity, and breakdown electric field adds to its better thermal and electronic properties.

In the last few years it has been recognized that nanostructured porous semiconductor networks show interesting optoelectrical properties different from those of bulk semiconductors. These properties are related to the presence of a three-dimensional (3-D) interfacial structure with a huge internal surface area and huge volume density of surface-localized electrons. At present, extensive research is devoted to nanostructured semiconductor networks. It is believed that such networks will play an important role in future (opto-) electronic devices (solar cells, light emitting diodes, chemical sensors, electrochromic devices, single electron transistors).

In recent years, porous silicon carbide has been of interest due to its more efficient luminescence compared to bulk SiC.[1] Also, electroluminescent and gas sensor devices based on porous SiC have been demonstrated.[2,3]

In order to use porous SiC in device application, the correlation between electrical characteristics and structural morphology of the porous layer must be understood. The goal of this work was to investigate the surface and pore morphology of 6H-SiC with respect to the effect of varying current density used during electrochemical anodization. The characterization technique used to study the surface and pore morphology has never been reported before.

Preparation and Characterization

Porous silicon carbide (por-SiC) samples were prepared using n-6H-SiC (0°8′ off axis) wafers from CREE Research Inc. This wafer was nitrogen doped and had a resistivity of 0.174 Ω cm. Photo-assisted electrochemical etching was performed on both the polished silicon-and carbon-terminated faces of the samples using a 150 W mercury (Hg) lamp and a mixture of hydrofluoric acid (HF) (1): ethanol (1) as electrolyte for a time period of 2-60 min. Prior to turning on the current, the sample arrangement in the Teflon cell was kept under the Hg lamp for 1 min. The counter electrode was a platinum wire positioned about 1 cm from the sample. The applied current density was between 10 and 80 mA/cm^2. Por-SiC samples were analyzed after ultrasonic cleaning in methanol for 10-20 min. Thicknesses of the porous layers were measured by the cylindrical grove technique. In order to study the porous structure beneath the surface, some samples were subjected to dry etching by reactive ion etching (RIE) to remove a thin (0.1-0.3 μm) surface layer. The RIE was performed in the March Instrument, Inc. system using a gas mixture (CF_4 + 15%O_2) at 150 W. A scanning electron microscope (SEM) was used to study the microstructure of the porous SiC surface layer.

In this work we have taken two batches of five samples each, and we are showing the recurring results for SEM images. For the plots, average results of both the experiments are considered.

Results and Discussion

Figure 1 shows the measured porous silicon carbide film thicknesses as a function of anodization time for both silicon (Si) and carbon (C) faces at current densities of 10 and 40 mA/cm^2. Each data point in these plots has been taken from the thickness measurements of different por-SiC samples processed under the same conditions but with anodization time as the only variable. The anodization time was varied from 5 to 60 min and from 2 to 10 min at a current density of 10 and 40 mA/cm^2, respectively. We limited the time of anodization to 10 min at current densities more than 40 mA/cm^2 because peeling of the porous layer occurs in these cases. It is clear that a por-SiC film grows linearly for these current densities during the first 10 min. After that, the growth rate becomes lower and the film thickness as a function of time might be interpolated by a parabolic curve. Based on the fact that the process of porous layer formation consists of two main reactions (oxidation and the oxide etching),[4] we may assume that the mechanism of anodization is similar to the kinetics of oxidation. During the initial period of anodization when the thickness of the porous layer is fairly thin, the limiting process of the porous layer growth is the reaction at the interface between the substrate and the porous layer. However, when the thickness of the porous layer becomes higher, then the growth rate is limited by the diffusion of electrolyte through the porous layer leading toward the interface. It leads to the lowering of the porous layer growth rate. Moreover, it is known that the oxidation rate of the Si-face is significantly less than that of the C face of a SiC crystal.[5] This explains the formation of thinner porous layer on the Si face compared to the C face at the same conditions.

The anodization rate appeared to be directly related to the current density used in these experiments. For the initial period (up to 10 min), the growth rate increases from 0.3 to 1.1 μm/min for the Si face and from 0.8 to 1.5 μm/min for the C face when the current

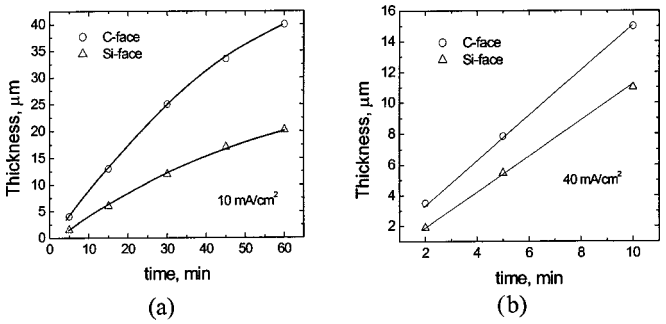

Figure 1. Thickness of porous layer as a function of time for current density of (a) 10 mA/cm^2 and (b) 40 mA/cm^2.

[z] E-mail: dast@engr.sc.edu

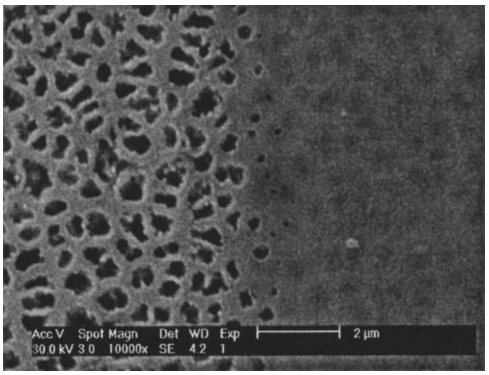

Figure 2. SEM image of porous SiC after 0.3 μm surface layer removal from half surface (on the left side).

density is increased from 10 to 40 mA/cm^2. It should be noted, that the anisotropic properties of SiC appear more clearly at lower current densities because the difference between the porous layer growth rate of Si and C faces is several times greater at current density of 10 mA/cm^2 than at current density of 40 mA/cm^2.

SEM analysis of an ''as-formed'' porous SiC surface could not reveal any characteristic pattern on it. It might be explained by the fact that the openings of the pores that propagate through the por-SiC layer have diameter on the surface of the order of 20 nm or less.[6] A similar porous layer structure is also observed in porous Si.[7] There were very thin surface layers with thickness less than 0.1 μm and pore diam in the order of 5-10 nm, which could barely be observed with SEM. These pores increase in diameter up to several hundreds of nanometers as they extend from surface to bulk. This led us to the idea of stripping of the skin layer to observe the bulk pore morphology. After removal of the surface layer of about 0.3 μm thick using RIE, the characteristic pattern of a porous structure could be observed. An SEM image of the porous SiC sample (current density of 40 mA/cm^2 for 5 min) after the removal of a thin layer from a half surface is shown in Fig. 2. This image is taken from the boundary region where the porous surface with a removed layer is on the left side and as-formed porous surface is on the right side. Note that the SEM applied electron accelerating voltage was 30 kV. This allowed the electrons to penetrate deeper into the substrate and reveal the porous structure, which is beneath the thin surface layer (see shadow on the right side of Fig. 1). As can be seen, the pore openings have irregular shapes with feature sizes varying from 0.3 to 0.7 μm. But, there is also a very narrow region at the edge of the removed layer where the pore openings have a circular shape with diam of less than 0.1 μm. Obviously, the thickness of the removed layer in this transition region was less than that in the region which is far enough from the boundary. It indicates that pore size enlarges with depth from several nanometers on the surface to several hundreds of nanometers at a depth of around 0.3 μm.

Figure 3 shows planar SEM images of por-SiC samples anodized at the current densities of 10, 20, 40, and 60 mA/cm^2 for 5 min after 0.1 μm surface layer removal. The SEM electron accelerating voltage in this case was 5 kV. Thus, electrons could not penetrate deep into the substrate to be able to reveal the porous structure, which is located deeper. However, in this case, the electrons could be accumulated at the sharp edges of the pore openings resulting in an appearance of the bright rings around the holes on the surface.

The lowest pore density of 3×10^7 cm^{-2} was obtained at the anodization current density of 10 mA/cm^2 (Fig. 3a). Pore diameter for this case was fairly uniform and varied from 250 to 300 nm. An increase of the current density to 20 mA/cm^2 leads to an increase of the pore density to 1×10^8 cm^{-2} and to the formation of pores with larger diam (300-400 nm) at the depth of 0.1 μm as well. A further double of the current density (up to 40 mA/cm^2) forms a porous network with the pore density of 1.5×10^8 cm^{-2}. More-

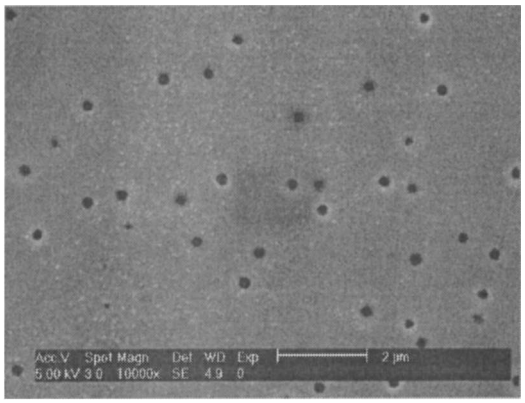

(a)

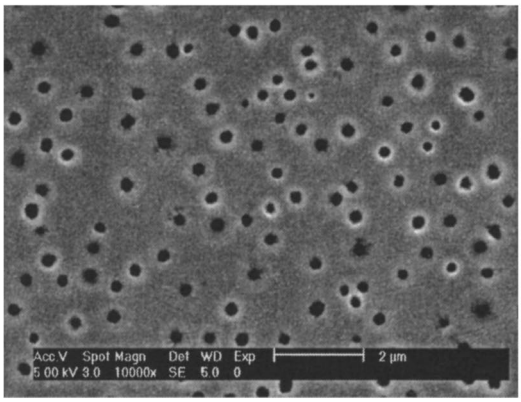

(b)

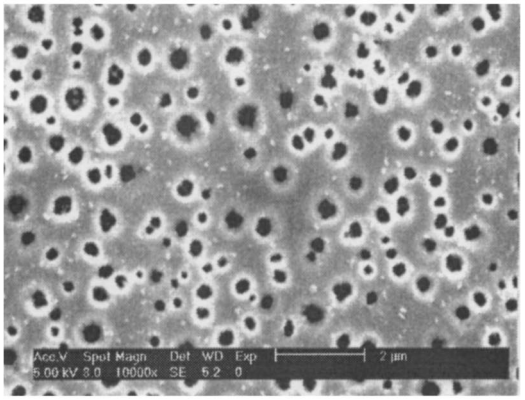

(c)

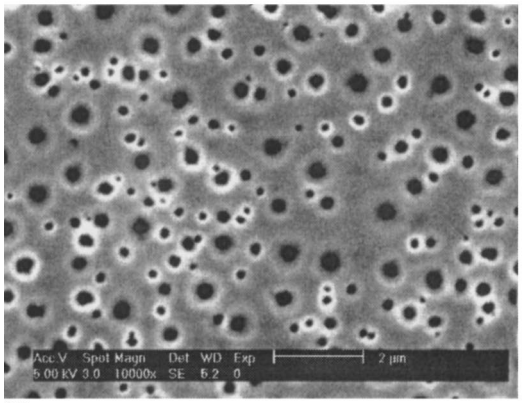

(d)

Figure 3. SEM image of porous SiC after 0.1 μm surface layer removal, anodized at different current densities: (a) 10 mA/cm^2, (b) 20 mA/cm^2, (c) 40 mA/cm^2, and (d) 60 mA/cm^2.

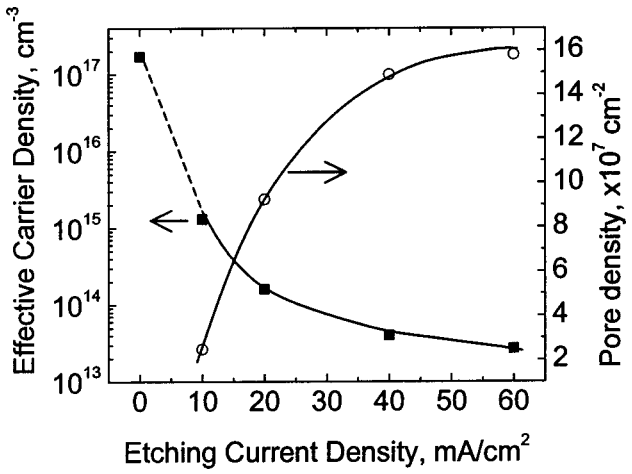

Figure 4. Effective carrier density (left scale) and pore density (right scale) *vs.* etching current density.

over, in this case, the pore openings have an irregular shape with feature size of 500 nm. A dependence of the pore density *vs.* the current density is plotted in Fig. 4 (right scale).

Electrical characterization of the formed porous SiC layers was implemented using capacitance-voltage (C-V) measurements of Schottky contacts by an annular mercury probe. Based on $1/C^2$-V curves, we could extract the effective carrier density in the porous layers anodized at different current densities. This curve is presented in Fig. 4 (left scale). We use the term ''effective'' to underline that we consider a porous layer comprising both voids (pores) where there are no carriers and the remaining single crystalline SiC lattice where the carrier density is equal to that of the initial substrate. The effective carrier density evidently should be proportional to the inverse porosity and/or pore density. The two plots in Fig. 4 clearly show that the effective carrier density extracted from the C-V characteristics and the pore density calculated based on SEM images are in a good agreement. Note that the initial substrate carrier concentration measured by the same CV method was 2×10^{17} cm^{-3} (shown in the plot at the zero current density), while the effective carrier density drops below 10^{14} cm^{-3} at current density of more than 20 mA/cm^2.

Conclusions

Porous SiC layers were obtained by electrochemical anodization of both the Si and C face of n-6H-SiC. Anisotropic properties of SiC result in different porous layer growth rates which were 0.3 *vs.* 0.8 μm/min at 10 mA/cm^2 and 1.1 *vs.* 1.5 at 40 mA/cm^2 for the Si and C faces, respectively. A characteristic porous structure could be observed using SEM after removal a thin (0.1-0.3 mm) surface layer by RIE. The effective carrier density in the porous layer extracted from the C-V characteristics and the pore density calculated based on SEM images were found to be in good correlation. The lowest effective carrier density in the porous layer was 3×10^{13} cm^{-3} after applied anodization current density of 60 mA/cm^2 for 5 min.

Acknowledgments

We are grateful to Dr. C. Wood for his interest and support of this research. This research was supported from ONR, grant no. N00014-01-10282. Also, the authors are grateful to Dr. Donggao for SEM measurements.

One of the authors, T. Das, assisted in meeting the publication costs of this article.

References

1. J. E. Spanier, G. S. Cargill III, I. P. Herman, S. Kim, D. R. Goldstein, A. D. Kurtz, and B. Z. Weiss, in *Advances in Microcrystalline and Nanocrystalline Semiconductors*, R. W. Collins, P. M. Fauchet, I. Shimizu, J. C. Vial, T. Shimada, and A. P. Alivisatos, Editors, in *MRS Symposia Proceedings* no. 452, p. 491, Materials Research Society, Pittsburgh, PA (1997).
2. H. Mimura, T. Matsumoto, and Y. Kanemitsu, *Appl. Phys. Lett.*, **65**, 3350 (1994).
3. V. B. Shields, M. A. Ryan, R. M. Williams, M. G. Spencer, D. M. Collins, and D. Zhang, in *Silicon Carbide and Related Materials, 1995*, *Institute of Physics Conference Proceedings*, S. Nakashima, H. Matsunami, S. Yoshida, and H. Harima, Editors, no. 142, Chap. 7, p. 1067, Institute of Physics, London (1996).
4. W. Shin, T. Hikosaka, W. E. Seo, H. S. Ahn, N. Sawaki, and K. Koumoto, *J. Electrochem. Soc.*, **145**, 2456 (1998).
5. S. Soloviev, T. Das, and T. S. Sudarshan, in *Technical Digest of the International Conference on SiC and Related Materials-ISCRM 2001*, Part 2, Vol. 389-393, p. 1113, Oct 28-Nov 2, 2001.
6. S. Zangooie and H. Arwin, *J. Electrochem. Soc.*, **148**, G297 (2001).
7. X. G. Zhang, *J. Electrochem. Soc.*, **138**, 3750 (1991).